

Review

Hydrothermal Crystal Growth of Piezoelectric α -Quartz Phase of AO_2 ($A = \text{Ge, Si}$) and MXO_4 ($M = \text{Al, Ga, Fe}$ and $X = \text{P, As}$): A Historical Overview

Olivier Cambon * and Julien Haines

Institut Charles Gerhardt Montpellier, Centre National de la Recherche Scientifique, Université de Montpellier, Ecole Nationale Supérieure de Chimie de Montpellier, Montpellier 34095 Cedex 05, France; julien.haines@umontpellier.fr

* Correspondence: olivier.cambon@umontpellier.fr; Tel.: +33-4-67-14-32-04

Academic Editors: Alain Largeteau and Mythili Prakasam

Received: 19 November 2016; Accepted: 25 January 2017; Published: 4 February 2017

Abstract: Quartz is the most frequently used piezoelectric material. Single crystals are industrially grown by the hydrothermal route under super-critical conditions (150 MPa–623 K). This paper is an overview of the hydrothermal crystal growth of the AO_2 and MXO_4 α -quartz isotypes. All of the studies on the crystal growth of this family of materials enable some general and schematic conclusions to be made concerning the influence of different parameters for growing these α -quartz-type materials with different chemical compositions. The solubility of the material is the main parameter, which governs both thermodynamic parameters, P and T, of the crystal growth. Then, depending on the chemistry of the α -quartz-type phase, different parameters have to be considered with the aim of obtaining the basic building units (BBU) of the crystals in solution responsible for the growth of the α -quartz-type phase. A schematic method is proposed, based on the main parameter governing the crystal growth of the α -quartz phase. All of the crystal growth processes have been classified according to four routes: classical, solute-induced, seed-induced and solvent-induced crystal growth.

Keywords: hydrothermal crystal growth; α -quartz isotypes; basic building units (BBU) of the crystal; nucleation; homo-epitaxy; hetero-epitaxy; solute; seed; solvent

1. Introduction

Hydrothermal growth is a natural process and occurs in the Earth's crust. Originally, this term was used to describe the dissolution of rocks and minerals by water, under elevated pressures and temperatures, and the crystallization of various inorganic phases. Beryl, calcite, and quartz are the well-known large crystals, which are extracted from the Earth. Due to the interest in such materials, the hydrothermal technique was used to produce industrially synthetic materials, like quartz, for electronic applications [1,2]. Synthetic beryl and calcite single crystals have also been grown hydrothermally [3–6]. The term hydrothermal is now used to describe crystallization processes using aqueous solvents in a closed vessel. Based on this approach, sub- or super-critical conditions have been used in the vessel, depending on the solvent. This paper presents a review of the hydrothermal synthesis of the α -quartz phase in $A^{IV}O_2$ ($A = \text{Si, Ge}$) and $M^{III}X^VO_4$ ($M = \text{Al, Ga}$ and $X = \text{P, As}$) compounds. The α -quartz type structure belongs to the $P3_121$ or $P3_221$ space group. AO_4 ($A = \text{Si}$ and/or Ge for SiO_2 , GeO_2 or $\text{Si}_{1-x}\text{Ge}_x\text{O}_2$), MO_4 , and XO_4 (for MXO_4) tetrahedral units are connected, forming a helical chain along the c axis (Figure 1). The α -quartz phase is stable at room temperature for all of the compounds except for GeO_2 , for which the α -quartz phase is stable at high temperatures from 1306 K up to the melting point at 1388 K (Table 1): the α -quartz-type phase of GeO_2 is a thermodynamic metastable phase at

room temperature. The stable phase of GeO_2 under ambient conditions is a rutile-type phase, in which the germanium is 6-fold coordinated.

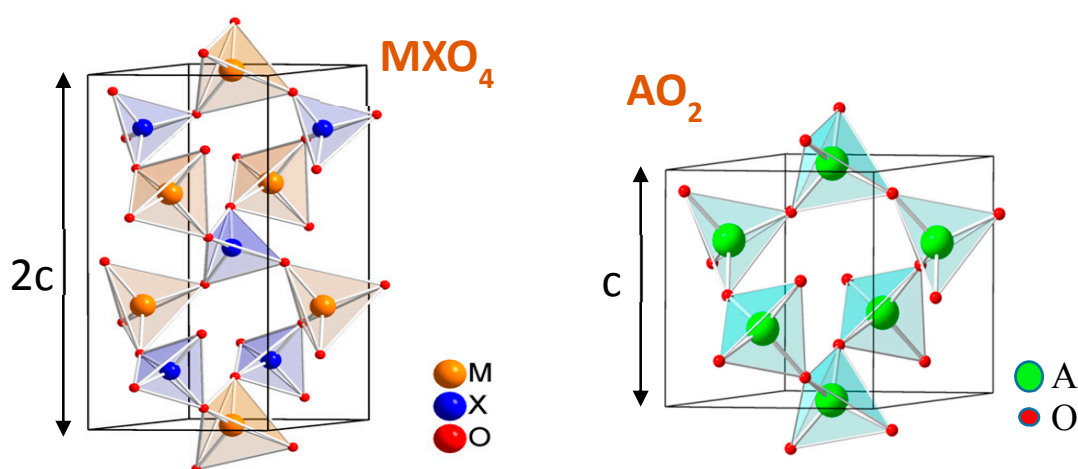


Figure 1. α -quartz structure of AO_2 ($A = \text{Si}, \text{Ge}$) and MXO_4 ($M = \text{Al}, \text{Ga}, \text{Fe}$ and $X = \text{P}, \text{As}$) materials.

Table 1. Polymorphism of the AO_2 and MXO_4 materials.

Compound	Phase Transitions								
SiO_2	α -Quartz	$\xrightleftharpoons{846 \text{ K}}$	β -Quartz	$\xrightleftharpoons{870 \text{ K}}$	Tridymite	$\xrightleftharpoons{1673 \text{ K}}$	β -Cristobalite	$\xrightleftharpoons{1983 \text{ K}}$	liquid
GeO_2			β -Rutile	$\xrightleftharpoons{1306 \text{ K}}$	α -Quartz	$\xrightleftharpoons{1388 \text{ K}}$	Liquid		
AlPO_4	α -Quartz	$\xrightleftharpoons{859 \text{ K}}$	β -Quartz	$\xrightleftharpoons{1088 \text{ K}}$	Tridymite	$\xrightleftharpoons{1298 \text{ K}}$	β -Cristobalite	$\xrightleftharpoons{1870 \text{ K}}$	liquid
FePO_4			α -Quartz	$\xrightleftharpoons{980 \text{ K}}$	β -Quartz	$\xrightleftharpoons{1513 \text{ K}}$	Liquid		
GaPO_4			α -Quartz	$\xrightleftharpoons{1206 \text{ K}}$	β -Cristobalite	$\xrightleftharpoons{1943 \text{ K}}$	Liquid		
GaAsO_4			α -Quartz	$\xrightleftharpoons{1303 \text{ K}}$	Chemical decomposition				

2. Hydrothermal Crystal Growth

Following the initial work of Gibbs [7] in 1878, and then that of Frenkel [8] in 1945, Burton, Cabrera, and Frank [9,10] studied the growth of a real crystal from the vapor phase. Thermodynamic equations have been established, which describe the crystal growth from a structural defect, like a screw-type dislocation. Numerous authors [11–13] have applied this theory to growth from solution. Cabrera and Levine [14] extended this approach to dissolution, which is the reverse phenomenon with respect to crystal growth. All of these studies were reconsidered by Johnston in 1962 [15]. Basically, in crystal growth from solution, the solute crystallizes when the concentration of the solute becomes higher than the concentration at equilibrium, termed solubility. The solubility is the main parameter for growing crystals from solutions. Hydrothermal crystal growth corresponds to crystal growth from solution in a closed vessel. Temperature and pressure are two important thermodynamic parameters, which have to be adjusted according to the solvent used. The first step is to find the adequate thermodynamic conditions for obtaining a good reactivity of the solvent with the solute. Then, for growing crystals of high quality, the experimental conditions have to be adjusted to modify the kinetics of the exchanges between the solid phase and the solvent. By using hydrothermal techniques, thermodynamic-stable and metastable phases can be grown. The main experimental parameters, which can be adjusted are the solvent, the presence or absence of a nucleus (or seed) and both thermodynamic parameters, P and T.

One of the most important questions, which has to be solved before starting a hydrothermal process, is the choice of which pressure domain the crystal growth process will be performed in. To answer to this question, the ability of the solvent to dissolve the chemical precursors and to

recrystallize the desired phase has to be considered. In a polar solvent like aqueous solutions, the dissolution process forms ionic species in solution and crystallization is due to the condensation of the ionic species to form a new crystal. In pure water (pH = 7), H^+ and OH^- species are present with a concentration of 10^{-7} M.

2.1. Hydrothermal Growth of $A^{IV}O_2$ ($A = Si, Ge$)

In the Earth, crystal growth of quartz occurs in water, which acts as the solvent under hydrothermal conditions. In the supercritical state, water is more aggressive due to the decrease in its ionic product [16] and the growth of quartz single crystals can take place, but with very slow kinetics. For the industrial production of quartz crystals, sodium hydroxide [17] or carbonate solutions [18] are used as mineralizers in order to increase the dissolution and the crystallization rate. Pure α -quartz SiO_2 ($x = 0$) is the material used by Pierre and Jacques Curie in their discovery of the piezoelectric effect. From 1940, the industrial demand for quartz rapidly increased in the world and industrial processes of hydrothermal growth were developed [19–23]. Subsequently, quartz material has been widely used for various electronic applications, like ultra-stable oscillators for space applications, which require quartz single crystals of very high crystalline quality. Numerous works have been devoted to improving the quality of the crystals [17,24–31]. Nevertheless, its intrinsic performances are limited at high temperatures, due to the presence of the α - β phase transition. A study of the instantaneous structure of quartz by total neutron scattering has shown that the gradual loss of the piezoelectric properties, starting at 523 K, is due to an important increase in dynamic disorder at high temperature [32].

Over the past thirty years, scientists have been trying to replace quartz with materials that have better piezoelectric properties. Several years ago, studies were performed with the aim of modifying the chemistry of quartz and improving the piezoelectric properties. In these materials, a linear dependence between the piezoelectric efficiency (electromechanical coupling coefficient k) and the structural distortion was found, described by the inter-tetrahedral bridging angle θ [33–36]. Recently, studies based on DFT calculations have determined the origin and mechanism of the piezoelectric effects in the α -quartz family. Another criterion based on the elastic compliance constants, rather than the degree of distortion, has been proposed to classify the α -quartz-type compounds according to their piezoelectric efficiency (Table 2) [37,38]. Due to a compatible size of the ionic radius ($R(Si^{4+}) = 0.26$ Å and $R(Ge^{4+}) = 0.39$ Å), Germanium atoms have been introduced in the quartz network by substituting Si with Ge atoms [39,40]. An experimental phase diagram was determined by Miller [41], under a pressure of 70 MPa. The highest molar percent observed in the quartz phase is 31%, at 973 K. Beyond this value, phase separation occurs and a pure rutile phase of GeO_2 appears. Based on this data, Ge-substituted quartz crystals with the α -quartz structure have been grown under super-critical conditions using Ni-Cr-based alloy autoclaves. Different parameters (nutrient, solvent, temperature, pressure) have been studied and centimeter-sized single crystals with a maximum value of $x = 0.23$ have been obtained [42]. The mechanism of dissolution under hydrothermal conditions (up to 150 MPa and 475 °C) was studied by in-situ X-ray absorption at the Ge K-edge [43]. The local structure around Ge atoms was found to be a 4-fold coordinated environment. In pure H_2O solvent, $Ge(OH)_4$ (aq) species are formed, while in NaOH aqueous solution, $GeO(OH)_3^-$ species are produced, which are at the origin of the precipitation of relatively insoluble sodium germanates $Na_4Ge_9O_{20}$, reducing the degree of Ge-substitution in the crystals. To avoid this phenomenon, the NaOH concentration of the solvent was reduced to 0.05 M and a dissolution temperature of above 723 K was used, allowing the nutrient to be dissolved, even if it transforms in the rutile phase. The α -quartz-type crystals were then studied by Raman scattering [44]. The Raman shift of the coupled A_1 mode at 464 cm^{-1} for pure quartz was found to be a linear function of the Ge-content. Moreover, it was shown that the dynamic disorder observed in quartz well below the α - β quartz phase transition is greatly reduced by Ge-substitution in the crystalline network. As a result, the phase transition temperature increases from 846 K for $x = 0$ to 1300 K for $x = 0.24$. The hydrothermal method has then been applied in bigger

autoclaves in order to grow larger single crystals (10 cm along the y -axis) [45]. Resonators have been manufactured from crystals with $x = 0.0375$ and in pure α -quartz ($x = 0$) for comparison. Piezoelectric measurements have shown that the piezoelectric signal remains measurable after annealing up to 818 K for pure SiO_2 , and up to 908 K for an Ge-substituted crystal with $x = 0.0375$. This result is in agreement with the previous Raman [44] study and the decrease of the dynamic disorder by substituting Si atoms with Ge. Non-linear optical properties have been also measured by using the Maker's fringes method. The non-linear optical coefficient $\chi_{11}^{(2)}$ increases with Ge-substitution: $\chi_{11}^{(2)} = 1.3(2)$ and $1.6(2) \text{ pmV}^{-1}$ for $x = 0.023$ and 0.028 , respectively, in comparison to 0.67 pmV^{-1} for pure quartz ($x = 0$). By growing a SiO_2 - GeO_2 mixed α -quartz-type phase, 4-fold coordination of germanium was stabilized in an alpha-quartz phase. The hydrothermal process is performed in the (P, T) stability range of the SiO_2 α -quartz phase and the quartz-seeds are also stable under these conditions.

Table 2. DFT calculated piezoelectric constants and coupling factors K_{11} and K_{26} .

Compound	SiO_2 [37]	GeO_2 [37]	AlPO_4 [38]	GaPO_4 [38]	GaAsO_4 [38]
e_{11} (C/m ²)	0.148	0.22	0.14	0.22	0.21
d_{11} (pC/N)	2.06	5.63	2.7	4.8	7.1
K_{26} (%)	11.70	20.40	12.50	19.70	21.90
K_{11} (%)	8.84	16.22	10.27	15.11	18.03

In the case of GeO_2 ($x = 1$), there have been a few publications on hydrothermal crystal growth. Different solvents were studied for dissolving the α -quartz-type phase of GeO_2 : H_2O [46] and different aqueous fluoride solutions [47]. In 1972, the crystal growth of the α -quartz phase of GeO_2 in its metastable domain, by the hydrothermal route, was carried out [48]. The gradient method was used with {0001} and {0111} quartz-seeds. The nutrient was a crystalline or amorphous powder and water was used as the solvent. Crystal growth is rapidly limited by the transformation of the nutrient to the stable rutile-type phase, which is quite insoluble under these conditions. The crystals obtained were of poor quality. In order to increase the solubility, different mineralizers (NH_4F , NaOH , LiF , LiCl) were added in solution [49,50]. In spite of an improvement in the transport of the chemical species, the nutrient was transformed to the relatively insoluble rutile phase of GeO_2 . To avoid the phase transformation of the nutrient, a new refluxed method [51] of growth was developed, which consists of generating in the autoclave successive recirculation of the solution. In this way, the nutrient of soluble α -quartz GeO_2 is not permanently in contact with the solution and the nutrient does not transform into the relatively insoluble rutile-type phase. Crystals were grown to a sufficient size (a few cm) in order to measure their physical properties, but the high $-\text{OH}$ content in the crystals prevents their use in piezoelectric device applications.

2.2. Hydrothermal Growth of $M^{\text{III}}X^{\text{V}}\text{O}_4$ ($M = \text{Al}, \text{Ga}, \text{Fe}; X = \text{P}, \text{As}$)

MXO_4 materials are built up of MO_4^{5-} and XO_4^{3-} tetrahedra. The latter are conjugated bases of acids and, consequently, the dissolution and crystal growth of MXO_4 compounds are often performed in acid solvents and sub-critical conditions (low P-T conditions) are used. Berlinite AlPO_4 is the only MXO_4 -type material found in nature [52,53].

2.2.1. AlPO_4 Single Crystals

Synthetic single crystals of berlinite were grown for the first time by Jahn and Kordes in 1953 [54]. In 1976, with the development of the telecommunication techniques, AlPO_4 single crystals became of high interest, because of their better piezoelectric properties, when compared to those of quartz [55,56]. It was even said that "berlinite could replace quartz". Numerous studies have been devoted to berlinite crystal growth [57–61]. In 1983, Chai developed a technique of seed lengthening by gluing. Large crystals (10 cm) were grown in H_3PO_4 acid solvent, at temperatures lower than 473 K and low

pressures (less than 20 bar), and by using a slow temperature increase. The process was protected by a US patent [62]. At the same time, new conditions of AlPO_4 crystal growth were studied in 4.5 M H_2SO_4 solvent at a laboratory scale ($T = 503$ K, $P < 2$ MPa), by using a reverse temperature gradient [63,64]. High quality single crystals were obtained with lower $-\text{OH}$ impurities and dislocation content [65]. This can lead to the development of new electronic devices, like resonators and filters [66,67]. For high frequency Bulk Acoustic Waves (BAW) filters, a controlled dissolution process of berlinite wafers was investigated. On the basis of the Burton Cabrera and Franck theory [10], applied to the dissolution mechanism [14], dissolution by using slightly under-saturated acidic solutions has been studied, leading to smooth surfaces without superficial defects, like etch pits [68–70]. Due to the difficulties in transferring the laboratory conditions of crystal growth to an industrial scale and due to the disappearance of the AlPO_4 dedicated application (IF filter for the mobile wireless technology), the industrial development of berlinite crystal growth was abandoned.

2.2.2. GaPO_4 Single Crystals

From 1990, GaPO_4 has been studied extensively because of its similar crystal growth process to AlPO_4 . Moreover, GaPO_4 was a very promising material with high expected piezoelectric properties. Different solvents were used: H_3PO_4 , H_2SO_4 , and mixtures have been the most studied [71–78]. As for AlPO_4 , the solubility of GaPO_4 is the reverse below 673 K. A seed lengthening process has been developed by splicing [79]. Structural defects like dislocations have been reduced by growing crystals successively along crossed directions [80]. It was shown that the $-\text{OH}$ content is reduced with low concentrated acid solution and at temperatures of crystallization higher than 673 K. GaPO_4 has been tested for manufacturing resonators and wide band filters [81]. As for AlPO_4 , a wet chemical-controlled dissolution process has been developed. Very smooth surfaces ($R_a = 0.02$ μm) have been obtained by using a basic solvent [82]. One of the most important benefits of GaPO_4 is the thermal stability of the piezoelectric α -quartz phase up to 1206 K. GaPO_4 -based resonators have been measured up to 1073 K and no degradation of the electrical parameters was observed below 973 K [83]. The instantaneous structure of GaPO_4 has been studied by total neutron scattering and the high degree of dynamic disorder above 973 K was linked to the decrease of the piezoelectric properties [84]. From 1997, GaPO_4 was industrially developed by the AVL-Piezocryst Company in Austria [85,86] for pressure sensor applications at high temperature in combustion engines and turbines. Very large crystals ($7 \times 15 \times 7$ cm) are grown from epitaxy on quartz-seeds [87] and by using a reverse temperature gradient.

2.2.3. GaAsO_4 Single Crystals

The structure of GaAsO_4 was refined by neutron and X-ray diffraction, from 15 K to 1073 K [88]. This study demonstrated the high thermal stability of the α -quartz phase with the highest degree of structural distortion in α -quartz materials leading to the prediction that GaAsO_4 would have the best piezoelectric properties in this family. Single crystals were grown for the first time by hydrothermal methods by using 11.5 M H_3AsO_4 as the solvent. High quality crystals with well-defined faces were obtained by nucleation [89]. The OH-defect content was quantified by infra-red spectroscopy, confirming the high crystalline quality of the material, thereby allowing the first physical characteristics, like the free-stress dielectric constants of GaAsO_4 , to be measured ($\epsilon_{11} = 8.5$, $\epsilon_{33} = 8.6$). Based on these first results, the electromechanical coupling factor was estimated to be 22%, the highest value in the α -quartz family by using the linear dependence between the electromechanical coupling factor k and the inter-tetrahedral bridging angle mentioned above. The first piezoelectric measurements on a centimeter-sized single crystal confirmed that gallium arsenate is the highest-performance piezoelectric material among α -quartz-type materials. Moreover, thermal gravimetric analysis, coupled with X-ray diffraction as a function of temperature, showed that GaAsO_4 with the α -quartz structure is stable up to 1303 K [90]. Total neutron scattering experiments, Raman spectroscopy and theoretical DFT calculations have shown that the absence of libration modes of the tetrahedra limits the dynamic disorder and

show that GaAsO₄ could be of high interest for piezoelectric applications at high temperatures [91]. Elastic constants have been measured by Brillouin spectroscopy [92]. The crystal growth process has been reviewed with the aim of increasing the crystal size by epitaxy on large seeds [93]. A new method was developed to synthesize the GaAsO₄ nutrient from GaAs as the starting material in a sulfuric acid solvent under oxidizing conditions. Centimeter-sized single crystals were grown from oriented GaPO₄ and AlPO₄ seeds. The role of the nature and orientation of the seeds and the influence of the solute supply on the growth rate were studied. Crystals of high quality were obtained with a low value of the infrared absorption coefficient α at 3300 cm⁻¹ ($\alpha = 0.067$ cm⁻¹), indicating a low –OH impurity content in the crystals. UV–vis–NIR spectrophotometry measurements on these crystals exhibit the highest value of birefringence in the α -quartz group with $\Delta n = 0.033$. The measured bandgap is 5.85 eV. Piezoelectric properties were measured on resonators. An electromechanical coupling coefficient of 20% with a quality factor of 3.2×10^{10} was obtained and the C₆₆ elastic constant was found to be 20 GPa. Finally, first-principle calculations of the second-order nonlinear optical properties of GaAsO₄, combined with measurements of its second harmonic generation (SHG) using the technique of Maker fringes, show that GaAsO₄ has a SHG efficiency between 7.1 (LDA) and 12.3 pm/V (GGA), which is in agreement with the experiments (7.5 ± 1.5 pm/V). Moreover, the high laser damage threshold (0.93 GW/cm²) makes α -quartz-type GaAsO₄ a bifunctional material for high temperature piezoelectric and for high power laser SHG applications [94].

2.2.4. α -quartz FePO₄

Hydrothermal crystal growth of α -quartz FePO₄ was never successful. Numerous studies [95–98] described the use of acidic solutions containing Fe³⁺ and PO₄³⁻ ions, but the phases obtained were hydrated phases of phosphosiderite, with a strengite-type FePO₄·nH₂O composition and giniite, Fe₃(PO₄)₂(OH)₂·nH₂O. After heating these phases at 873 K, they transform to the α -quartz phase of FePO₄ [97–99]. FePO₄ with the α -quartz structure was studied by Raman scattering [100].

2.2.5. M'(1-x)M_xPO₄ Solid Solutions

The interest in developing solid solutions is to design materials, which have tunable physical properties that depend on the chemical composition (x).

Al_{1-x}Ga_xPO₄

Solid solutions exist between AlPO₄ and GaPO₄ [101–104]. Al_{1-x}Ga_xPO₄ powders were synthesized by hydrothermal methods. Solutions of AlPO₄ and GaPO₄ in sulfuric acid were initially individually prepared and then mixed together in a different ratio, due to differences in solubility, placed in a Polytetrafluoroethylene-lined autoclave and then heated in order to induce crystallization [105]. In this case, sulfuric acid is a common solvent for the two end-members of the pseudo-binary, which is a favorable condition for inducing nucleation and crystal growth. The instantaneous structures of Al_{1-x}Ga_xPO₄ solid solutions were studied as a function of temperature and chemical composition (x) [106]. It was shown that the dynamic disorder in the oxygen sub-lattice decreases with the Ga-content.

Ga_{1-x}Fe_xPO₄

The α -quartz phase of FePO₄ has never been directly synthesized under hydrothermal conditions, due to the six-fold coordination of the Fe³⁺ ions in solution. One of the motivations to synthesize Ga_{1-x}Fe_xPO₄-mixed crystals is to induce the crystallization of an α -quartz phase with four-fold coordinated iron atoms, from solutions under hydrothermal conditions. As for Al_{1-x}Ga_xPO₄, different amounts of FePO₄·2H₂O and GaPO₄ powder were dissolved in 5 M H₂SO₄, for 48 h. The solution obtained was then heated in a PTFE-lined autoclave at 230 °C for ~10 days. After rapid cooling, single crystals were obtained [100]. The highest value of iron content was $x = 0.11$ [107]. The mechanism of crystal growth was studied by in situ X-ray absorption spectroscopy (XAS) at the Fe K-edge [108].

It was shown that the crystallization of pure α -quartz-type FePO_4 is not possible due to the high stability of the hexa-aqua complexes $[\text{Fe}(\text{H}_2\text{O})_6]^{3+}$ without any FeO_4 entities. In the presence of Ga^{3+} ions in solution, the growth of a mixed phase of α -quartz-type $\text{Ga}_{1-x}\text{Fe}_x\text{PO}_4$ is possible with x up to 0.23. A mechanism was proposed based on the formation of mixed (iron/gallo)-phosphate complexes at the solid-liquid interface, which are at the origin of the nuclei for crystallization. In this way, the 4-fold coordination of Fe^{3+} is chemically induced by the presence of Ga^{3+} cations in solution (solute-induced crystal growth).

3. General Discussion about Hydrothermal Crystal Growth Conditions

Various conditions need to be selected for hydrothermal growth of α -quartz phases of AO_2 and MXO_4 materials. A schematic summary of different conditions is given in Figure 2. Thermodynamic P-T conditions first have to be determined to ensure the dissolution of the material. This step defines the type of the autoclave required (LP/LT or HP/HT autoclave). Then, different parameters have to be taken into account, according to the type of crystal growth.

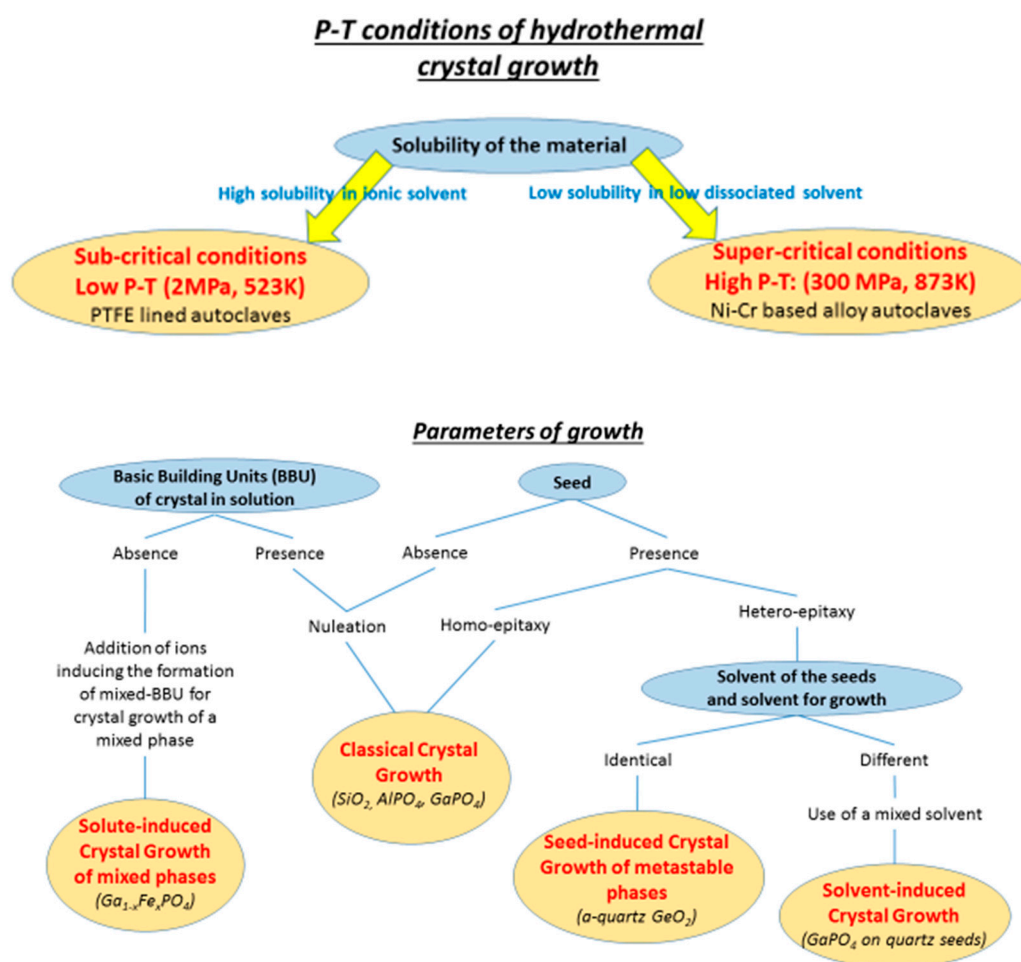


Figure 2. Schematic summary of different parameters governing the hydrothermal crystal growth of the α -quartz type materials.

Classical crystal growth: In the case of nucleation, the crystal growth is only due to the species present in the solution. To obtain nuclei of the desired structure in the solution, the basic building units of the crystal have to be present in the solution. This is the most common case for thermodynamically-stable phases, where the crystallization and the dissolution phenomena occur.

Pure phases (SiO_2 , AlPO_4 , GaPO_4 , GaAsO_4) and solid-solutions ($\text{Al}_{1-x}\text{Ga}_x\text{PO}_4$) can be grown by nucleation in the same solvent.

Solute-induced crystal growth: For chemical elements, which do not adopt the basic building unit of the structure of the crystal in the solution, it is impossible to grow a pure phase. This is the case of α -quartz-type FePO_4 , which has never been directly crystallized under hydrothermal conditions, because Fe^{3+} ions are 6-fold coordinated in aqueous solvent and only hydrated phases are obtained. To force Fe^{3+} into a 4-fold coordination, it is necessary to add a 4-fold coordinated element like Ga^{3+} into the solution. In this way, only solid-solutions such as $\text{Ga}_{1-x}\text{Fe}_x\text{PO}_4$ are obtained. Nucleation can be termed a solute-induced crystal growth process. Moreover, it is impossible to obtain nuclei of a thermodynamically-metastable phase. This is the case for the α -quartz phase of GeO_2 . Crystals of α -quartz GeO_2 are only obtained by epitaxy (see below).

In the case of the crystal growth from a pre-existing seed, termed epitaxy, the seed could be of the same composition and structure of the crystal, termed homo-epitaxy, or of different composition and structure, termed hetero-epitaxy. Homo-epitaxy is the most common case. This process is the step after the classical nucleation step in the same solvent described above. This is the most favorable case for obtaining large single crystals without structural defects like twins, cracks, or dislocations. All crystal growth processes tend towards this case.

Seed-induced crystal growth: In the case of no pre-existing seed, hetero-epitaxy has to be developed, since nucleation is impossible. This is the case for α -quartz GeO_2 growth, where crystals were grown by hetero-epitaxy on α -quartz SiO_2 seeds. The crystal growth can be termed seed-induced crystal growth. Indeed, for all hydrothermal conditions tested, the α -quartz-type GeO_2 phase grows only on the quartz-seeds, while GeO_2 transforms rapidly to the rutile phase in the other parts of the autoclave [109]. In the case of $\text{Si}_{1-x}\text{Ge}_x\text{O}_2$ solid solution, the crystal growth is performed at HP and HT ($T > 723$ K), enabling the dissolution of GeO_2 even if it transforms to the rutile phase. In this way and due to the presence of α -quartz SiO_2 seeds, the crystal growth of α -quartz-type $\text{Si}_{1-x}\text{Ge}_x\text{O}_2$ is possible.

Solvent-induced crystal growth: The hetero-epitaxy process is also used when the pre-existing seeds are too small. This is the case when growing very large GaPO_4 crystals for industrial applications. The hetero-epitaxy process has been developed from large pre-existing α -quartz SiO_2 seeds. To perform this kind of process, a mixed solvent has been used by adding fluoride ions into the GaPO_4 solvent, in order to induce a small amount of dissolution of the SiO_2 seeds, before the start of the growth of the α -quartz-type GaPO_4 phase. In this case, the crystal growth of GaPO_4 on quartz-seeds is induced by the solvent (solvent-induced crystal growth).

4. Conclusions

All of the different studies on the hydrothermal crystal growth of the α -quartz phase of $A^{\text{IV}}\text{O}_2$ ($A^{\text{IV}} = \text{Ge}, \text{Si}$) and MXO_4 ($M = \text{Al}, \text{Ga}, \text{Fe}$ and $X = \text{P}, \text{As}$) compounds allow us to review the different conditions of hydrothermal crystal growth. Depending on the thermodynamic stability and the chemistry of the α -quartz phases, the thermodynamic conditions are selected and the different process parameters inducing crystal growth allow the process to be classified as “classical”, “solute-induced”, “seed-induced” or “solvent-induced” crystal growth.

Author Contributions: Olivier Cambon and Julien Haines conceived the research and wrote the paper.

Conflicts of Interest: The authors declare no conflict of interest.

References

1. Schaffthault, K.F.E. Gelehrte Anzeigen Bayer. *Akad* **1845**, *20*, 557.
2. Spezia, G. Sull accrescimento del quarzo. *Atti Accad. Sci. Torino* **1900**, *35*, 95–107.
3. Kinloch, D.R.; Belt, R.F.; Puttbach, R.C. Hydrothermal growth of calcite in large autoclaves. *J. Cryst. Growth* **1974**, *24*, 610–613. [[CrossRef](#)]

4. Kikuta, K.; Hirano, S. Hydrothermal growth and dissolution behavior of calcite single-crystal in nitrate solutions. *J. Cryst. Growth* **1990**, *99*, 895–899. [[CrossRef](#)]
5. Shigley, J.E.; McClure, S.F.; Cole, J.E.; Koivula, J.I.; Lu, T.J.; Elen, S.; Demianets, L.N. Hydrothermal synthetic red beryl from institute of crystallography, Moscow. *Gems Gemol.* **2001**, *37*, 42–55. [[CrossRef](#)]
6. Demianets, L.N.; Ivanov-Shitz, A.K.; Gainutdinov, R.V. Hydrothermal growth of beryl single crystals and morphology of their singular faces. *Inorg. Mater.* **2006**, *42*, 989–995. [[CrossRef](#)]
7. Gibbs, J.W. *Collected Works*; Longmans Greenand Co.: London, UK, 1878.
8. Frenkel, J. Importance of steps and kink sites in crystal growth. *J. Phys. USSR* **1945**, *9*, 302.
9. Burton, W.K.; Cabrera, N. Crystal growth and surface structure. *Discuss. Faraday Soc.* **1949**, *5*, 33. [[CrossRef](#)]
10. Burton, W.K.; Cabrera, N.; Frank, F.C. The growth of crystals and the equilibrium structure of their surfaces. *Philos. Trans. Soc. Lond.* **1951**, *A243*, 299–358. [[CrossRef](#)]
11. Bennema, P. Analysis of crystal growth models for slightly supersaturated solutions. *J. Cryst. Growth* **1967**, *1*, 278–286. [[CrossRef](#)]
12. Gilmer, G.H.; Bennema, P. Simulation of crystal growth with surface diffusion. *J. Appl. Phys.* **1972**, *43*, 1347. [[CrossRef](#)]
13. Sunagawa, I.; Bennema, P. Morphology of growth spirals, theoretical and experimental. In *Preparation and Properties of Solid State Materials*; Wilcox, W.A., Ed.; Marcel Dekker: New York, NY, USA, 1982; Volume 7, pp. 1–129.
14. Cabrera, N.; Levine, M.M. On the dislocation theory of evaporation of crystals. *Philos. Mag.* **1955**, *1*, 450–458. [[CrossRef](#)]
15. Jonhston, W.G. Dislocation etch pits in non-metallic crystals. *Prog. Ceram. Sci.* **1962**, *2*, 1–75.
16. Marshall, W.L.; Franck, E.U. Ion product of water substance, 0–1000 °C, 1–10,000 bars new international formulation and its background. *J. Phys. Chem. Ref. Data* **1981**, *10*, 295–304. [[CrossRef](#)]
17. Buisson, X.; Arnaud, R. Hydrothermal growth of quartz crystals in industry. Present status and evolution. *J. Phys. IV* **1994**, *4*, 25–32. [[CrossRef](#)]
18. Sawyer, B. Q capability indications from infrared-absorption measurements for Na₂CO₃ process cultured quartz. *IEEE Trans. Sonics Ultrason.* **1972**, *19*, 41–44. [[CrossRef](#)]
19. Nacken, R. Hydrothermal syntheses als grundlage für zuchtung von quartzkristallen. *Chemiker Zeitung* **1950**, *74*, 745–749.
20. Laudise, R.A. Kinetics of hydrothermal quartz crystallization. *J. Am. Chem. Soc.* **1959**, *81*, 562–566. [[CrossRef](#)]
21. Laudise, R.A.; Ballman, A.A. Solubility of quartz under hydrothermal conditions. *J. Phys. Chem.* **1961**, *65*, 1396–1400. [[CrossRef](#)]
22. King, J.C.; Laudise, R.A.; Ballman, A.A. Improvement of mechanical Q of quartz by addition of impurities to growth solution. *J. Phys. Chem. Solids* **1962**, *23*, 1019–1921. [[CrossRef](#)]
23. Laudise, R.A.; Kolb, E.D. Hydrothermal synthesis of single crystals. *Endeavour* **1969**, *28*, 114–117.
24. Barns, R.L.; Freeland, P.E.; Kolb, E.D.; Laudise, R.A.; Patel, J.R. Dislocation-free and low-dislocation quartz prepared by hydrothermal crystallization. *J. Cryst. Growth* **1978**, *43*, 676–686. [[CrossRef](#)]
25. Laudise, R.A.; Barns, R.L. Perfection of quartz and its connection to crystal-growth. *IEEE Trans. Ultrason. Ferroelectr. Freq. Control* **1988**, *35*, 277–287. [[CrossRef](#)] [[PubMed](#)]
26. Zarka, A.; Lin, L.; Buisson, M. Influence of seeds on the density of dislocations produced during the growth of synthetic quartz. *J. Cryst. Growth* **1982**, *57*, 466–467. [[CrossRef](#)]
27. Yoshimura, M.; Byrappa, K. Hydrothermal processing of materials: Past, present and future. *J. Mater. Sci.* **2008**, *43*, 2085–2103. [[CrossRef](#)]
28. Demazeau, G. Solvothermal Processes: Definition, key factors governing the involved chemical reactions and new trends. *Z. Naturforsch. B* **2010**, *65*, 999–1006. [[CrossRef](#)]
29. McMillen, C.D.; Kolis, J.W. Bulk single crystal growth from hydrothermal solutions. *Philos. Mag.* **2012**, *92*, 2686–2711. [[CrossRef](#)]
30. Demazeau, G.; Largeteau, A. Hydrothermal/Solvothermal crystal growth: An old but adaptable process. *Z. Anorg. Allg. Chem.* **2015**, *641*, 159–163. [[CrossRef](#)]
31. McMillen, C.D.; Kolis, J.W. Hydrothermal synthesis as a route to mineralogically-inspired structures. *Dalton Trans.* **2016**, *45*, 2772–2784. [[CrossRef](#)] [[PubMed](#)]
32. Haines, J.; Cambon, O.; Keen, D.A.; Tucker, M.G.; Dove, M.T. Structural disorder and loss of piezoelectric properties in alpha-quartz at high temperature. *Appl. Phys. Lett.* **2002**, *81*, 2968–2970. [[CrossRef](#)]

33. Philippot, E.; Goiffon, A.; Ibanez, A.; Pintard, M. Structure Deformations and Existence of the α - β Transition in MXO_4 Quartz-like Materials. *J. Solid State Chem.* **1994**, *110*, 356. [[CrossRef](#)]
34. Philippot, E.; Palmier, D.; Pintard, M.; Goiffon, A. A general survey of quartz and quartz-like materials: Packing distortions, temperature, and pressure effects. *J. Solid State Chem.* **1996**, *123*, 1–13. [[CrossRef](#)]
35. Haines, J.; Chateau, C.; Leger, J.M.; Marchand, R. The use of composition and high pressure to extend the range of alpha-quartz isotypes. *Ann. Chim. Sci. Mater.* **2001**, *26*, 209–216. [[CrossRef](#)]
36. Haines, J.; Cambon, O.; Philippot, E.; Chapon, L.; Hull, S. A neutron diffraction study of the thermal stability of the alpha-quartz-type structure in germanium dioxide. *J. Solid State Chem.* **2002**, *166*, 434–441. [[CrossRef](#)]
37. Hermet, P. Piezoelectric response in alpha-quartz-Type GeO_2 . *J. Phys. Chem. C* **2016**, *120*, 126–132. [[CrossRef](#)]
38. Hermet, P.; Aubry, J.P.; Haines, J.; Cambon, O. Origin and mechanism of the piezoelectricity in a-quartz-type $M^{III}X^VO_4$ compounds ($M = B, Al, Ga; X = P, As$). *J. Phys. Chem. C* **2016**, *120*, 26645–26651. [[CrossRef](#)]
39. Passaret, M.; Regreny, A.; Bayon, J.F.; Aumont, R.; Toudic, Y. Recrystallization of TiO_2 , GeO_2 , SiO_2 , $Si_{(1-x)}Ge_xO_2$ in fluorinated hydrothermal solutions. *J. Cryst. Growth* **1971**, *13*, 524.
40. Balitsky, V.S.; Balitsky, D.V.; Nekrasov, A.N.; Balitskaya, L.V. Growth and characterization of $Si_xGe_{1-x}O_2$ solid solution single crystals with quartz structure. *J. Cryst. Growth* **2005**, *275*, E807–E811. [[CrossRef](#)]
41. Miller, W.S.; Roy, R.; Shafer, E.C.; Dache, F. System GeO_2 - SiO_2 . *Am. Mineral.* **1963**, *48*, 1024.
42. Ranieri, V.; Darracq, S.; Cambon, M.; Haines, J.; Cambon, O.; Largeteau, A.; Demazeau, G. Hydrothermal growth and structural studies of $Si_{(1-x)}Ge_xO_2$ single crystals. *Inorg. Chem.* **2011**, *50*, 4632–4639. [[CrossRef](#)] [[PubMed](#)]
43. Ranieri, V.; Haines, J.; Cambon, O.; Levelut, C.; Le Parc, R.; Cambon, M.; Hazemann, J.L. In Situ X-ray absorption spectroscopy study of $Si_{1-x}Ge_xO_2$ dissolution and Germanium aqueous speciation under hydrothermal conditions. *Inorg. Chem.* **2012**, *51*, 414–419. [[CrossRef](#)] [[PubMed](#)]
44. Ranieri, V.; Bourgogne, D.; Darracq, S.; Cambon, M.; Haines, J.; Cambon, O.; Leparç, R.; Levelut, C.; Largeteau, A.; Demazeau, G. Raman scattering study of alpha-quartz and $Si_{1-x}Ge_xO_2$ solid solutions. *Phys. Rev. B* **2009**, *79*, 224304. [[CrossRef](#)]
45. Clavier, D.; Prakasam, M.; Largeteau, A.; Boy, J.J.; Hehlen, B.; Cambon, M.; Hermet, P.; Haines, J.; Cambon, O. Piezoelectric and non-linear optical properties of alpha-quartz type $Si_{1-x}Ge_xO_2$ single crystals. *Crystengcomm* **2016**, *18*, 2500–2508. [[CrossRef](#)]
46. Kosova, T.B.; Demyanets, L.N.; Uvarova, T.G. Study of germanium dioxide solubility in water at the 25–300-Degrees-C. *Zhurnal Neorganicheskoi Khimii* **1987**, *32*, 768–772.
47. Demianets, L.N. Hydrothermal synthesis of new compounds. *Prog. Cryst. Growth Charact.* **1990**, *21*, 299–355. [[CrossRef](#)]
48. Roy, R.; Theokrit, S. Crystal growth of metastable phases. *J. Cryst. Growth* **1972**, *12*, 69–72. [[CrossRef](#)]
49. Balitsky, V.S.; Mahina, I.B. Patent N 461551, 1974. (In Russian)
50. Kosova, T.B.; Demianets, L.N. Hydrothermal chemistry and growth of hexagonal germanium dioxide. In *Growth of Crystals*; Springer: New York, NY, USA, 1991; Volume 16, pp. 81–94.
51. Balitsky, D.V.; Balitsky, V.S.; Pisarevsky, Y.V.; Philippot, E.; Silvestrova, O.Y.; Pushcharovsky, D.Y. Growth of germanium dioxide single crystals with alpha-quartz structure and investigation of their crystal structure, optical, elastic, piezoelectric, dielectric and mechanical properties. *Ann. Chim. Sci. Mater.* **2001**, *26*, 183–192. [[CrossRef](#)]
52. Blomstrand, C.W. *Om Westana Mineralier, Öfersigt at Kongliga Vetenskaps-Akademiens Handlingar*; P. A. Norstedt & Söner: Stockholm, Sweden, 1868.
53. Onac, B.P.; White, W.B. First reported sedimentary occurrence of berlinite ($AlPO_4$) in phosphate-bearing sediments from Cioclovina Cave, Romania. *Am. Mineral.* **2003**, *88*, 1395–1397. [[CrossRef](#)]
54. Jahn, V.W.; Kordes, E. Hydrothermal synthesis of large aluminum phosphate crystals. *Chem. Earth* **1953**, *70*, 75.
55. Stanley, J.M. Hydrothermal synthesis of large aluminum phosphate crystals. *Ind. Eng. Chem.* **1954**, *468*, 1684–1689. [[CrossRef](#)]
56. Chang, Z.P.; Barsch, G.R. Elastic constants and thermal expansion of berlinite. *IEEE Trans. Sonics Ultrason.* **1976**, *23*, 127–130. [[CrossRef](#)]
57. Kolb, E.D.; Grenier, J.C.; Laudise, R.A. Solubility and Growth of $AlPO_4$ in a hydrothermal solvent: HCl. *J. Cryst. Growth* **1981**, *51*, 178–182. [[CrossRef](#)]

58. Kolb, E.D.; Laudise, R.A. Pressure volume temperature behavior in the system $\text{H}_2\text{O}-\text{H}_3\text{PO}_4-\text{AlPO}_4$ and its relationship to the hydrothermal growth of AlPO_4 . *J. Cryst. Growth* **1982**, *56*, 83–92. [[CrossRef](#)]
59. Byrappa, K.; Venkatachalapathy, V.; Puttaraj, B. Crystallization of aluminum ortho-phosphate. *J. Mater. Sci.* **1984**, *19*, 2855–2862. [[CrossRef](#)]
60. Laudise, R.A. Hydrothermal synthesis of inorganic solids. *Abstr. Pap. Am. Chem. Soc.* **1985**, *189*, 48.
61. Byrappa, K. Recent progress in the growth and characterization of aluminum orthophosphate crystals. *Prog. Cryst. Growth Charact.* **1990**, *21*, 199–254. [[CrossRef](#)]
62. Chai, B.H.T. Hydrothermal crystal growing process and apparatus. Patent US 4382840, 10 May 1983.
63. Goiffon, A.; Jumas, J.C.; Avinens, C.; Philippot, E. Improving Berlinite crystal quality. Solubility and growth of Berlinite in sulfuric-acid. *Rev. Chim. Miner.* **1987**, *24*, 593–604.
64. Jumas, J.C.; Goiffon, A.; Capelle, B.; Zarka, A.; Doukhan, J.C.; Schwartzel, J.; Detaint, J.; Philippot, E. Crystal growth of Berlinite, AlPO_4 —Physical characterization and comparison with Quartz. *J. Cryst. Growth* **1987**, *80*, 133–148. [[CrossRef](#)]
65. Philippot, E.; Goiffon, A.; Maurin, M.; Detaint, J.; Schwartzel, J.C.; Toudic, Y.; Capelle, B.; Zarka, A. Evaluation of high-quality Berlinite crystals grown in sulfuric-acid medium. *J. Cryst. Growth* **1990**, *104*, 713–726. [[CrossRef](#)]
66. Detaint, J.; Poignan, H.; Toudic, Y. Experimental thermal behavior of berlinite resonators. In *34th Symposium on Frequency Control*; IEEE: Munchen, Germany, 1980; pp. 28–30.
67. Detaint, J.; Philippot, E.; Jumas, J.C.; Schwartzel, J.; Zarka, A.; Capelle, B.; Doukhan, J.C. Crystal growth, physical characterization and BAW devices applications of berlinite. In *Proceedings of the 3rd Annual Frequency Control Symposium*, Philadelphia, PA, USA, 29–31 May 1985.
68. Philippot, E.; Goiffon, A.; Maurin, M.; Cambon, O.; Ibanez, A.; Aubry, J.P. Procédé de Dissolution d'un Matériau Cristallin. Patent WO 1992009110 A1, 29 May 1992.
69. Cambon, O.; Goiffon, A.; Ibanez, A.; Philippot, E. Kinetics and dissolution mechanism of berlinite, AlPO_4 , in acid medium. *Eur. J. Sol. State Inorg.* **1992**, *29*, 547–561.
70. Cambon, O.; Goiffon, A.; Ibanez, A.; Philippot, E. Controlled dissolution of crystals: Application to Berlinite ($\alpha\text{-AlPO}_4$), a piezoelectric material. *J. Solid State Chem.* **1993**, *103*, 240–252. [[CrossRef](#)]
71. Hirano, S.; Miwa, K.; Naka, S. Hydrothermal synthesis of gallium ortho-phosphate crystals. *J. Cryst. Growth* **1986**, *79*, 215–218. [[CrossRef](#)]
72. Philippot, E.; Ibanez, A.; Goiffon, A.; Cochez, M.; Zarka, A.; Capelle, B.; Schwartzel, J.; Detaint, J. A quartz-like material—Gallium Phosphate (GaPO_4): Crystal growth and characterization. *J. Cryst. Growth* **1993**, *130*, 195–208. [[CrossRef](#)]
73. Cochez, M.; Foulon, J.D.; Ibanez, A.; Goiffon, A.; Philippot, E.; Capelle, B.; Zarka, A.; Schwartzel, J.; Detaint, J. Crystal growth and characterizations of α -quartz like material: GaPO_4 . *J. Phys. IV* **1994**, *4*, 183–188. [[CrossRef](#)]
74. Cochez, M.; Ibanez, A.; Goiffon, A.; Philippot, E. Crystal growth and infrared characterization of GaPO_4 in phospho-sulfuric media. *Eur. J. Sol. State Inorg.* **1993**, *30*, 509–519.
75. Palmier, D.; Goiffon, A.; Capelle, B.; Detaint, J.; Philippot, E. Crystal growth and characterizations of quartz-like material: Gallium phosphate (GaPO_4). *J. Cryst. Growth* **1996**, *166*, 347–353. [[CrossRef](#)]
76. Yot, P.; Palmier, D.; Cambon, O.; Goiffon, A.; Pintard, M.; Philippot, E. Crystal growth and characterization of an alpha-quartz-like piezoelectric material, gallium orthophosphate. *Ann. Chim. Sci. Mater.* **1997**, *22*, 679–682.
77. Cambon, O.; Yot, P.; Balitsky, D.; Goiffon, A.; Philippot, E.; Capelle, B.; Detaint, J. Crystal growth of GaPO_4 , a very promising material for manufacturing BAW devices. *Ann. Chim. Sci Mater.* **2001**, *26*, 79–84. [[CrossRef](#)]
78. Yot, P.; Cambon, O.; Balitsky, D.; Goiffon, A.; Philippot, E.; Capelle, B.; Detaint, J. Advances in crystal growth and characterizations of gallium orthophosphate, GaPO_4 . *J. Cryst. Growth* **2001**, *224*, 294–302. [[CrossRef](#)]
79. Yot, P. Matériaux piezoelectriques $\text{M}^{\text{III}}\text{X}^{\text{V}}\text{O}_4$ avec $\text{M} = \text{Al}, \text{Ga}, \text{Fe}$ et $\text{X} = \text{P}, \text{As}$ isotopes du quartz alpha: Etude structurale comparée et prévision des propriétés—Maîtrise de la croissance cristalline de l'orthophosphate de gallium, Université de Montpellier, Montpellier, France, 1999.
80. Capelle, B.; Zarka, A.; Schwartzel, J.; Detaint, J.; Philippot, E.; Denis, J.P. Characterization of piezoelectric materials—old and new Crystals. *J. Phys. IV* **1994**, *4*, 123–134. [[CrossRef](#)]

81. Detaint, J.; Capelle, B.; Cambon, O.; Philippot, E. Gallium phosphate plane resonators and filters. In Proceedings of the 2003 IEEE International Frequency Control Symposium & Pda Exhibition Jointly with 17th European Frequency and Time Forum, Tampa, FL, USA, 4–8 May 2003; pp. 679–687.
82. Prudhomme, N.; Flaud, V.; Papet, P.; Cambon, O.; Zaccaro, J.; Ibanez, A. Design of high frequency GaPO₄ BAW resonators by chemical etching. *Sens. Actuators B Chem.* **2008**, *131*, 270–278. [[CrossRef](#)]
83. Cambon, O.; Haines, J.; Fraysse, G.; Keen, D.A.; Tucker, M.G. Piezoelectric properties at high temperature in alpha-quartz materials. *J. Phys. V* **2005**, *126*, 27–30.
84. Haines, J.; Cambon, O.; Prudhomme, N.; Fraysse, G.; Keen, D.A.; Chapon, L.C.; Tucker, M.G. High-temperature, structural disorder, phase transitions, and piezoelectric properties of GaPO₄. *Phys. Rev. B* **2006**, *73*, 014103. [[CrossRef](#)]
85. Krempf, P.W.; Krispel, F.; Wallnofer, W. Industrial development and prospects of GaPO₄. *Ann. Chim. Sci. Mater.* **1997**, *22*, 623–626.
86. Reiter, C.; Thanner, H.; Wallnofer, W.; Krempf, P.W. Properties of GaPO₄ thickness shear resonators. *Ann. Chim. Sci. Mater.* **1997**, *22*, 633–636.
87. Krempf, P.; Voborsky, G.; Posch, U.; Wallnofer, W. Hydrothermal Process for Growing Large Crystals or Crystal Layers. U.S. Patent 5375556, 27 December 1994.
88. Philippot, E.; Armand, P.; Yot, P.; Cambon, O.; Goiffon, A.; McIntyre, G.J.; Bordet, P. Neutron and X-ray structure refinements between 15 and 1073 K of piezoelectric gallium arsenate, GaAsO₄: Temperature and pressure behavior compared with other alpha-quartz materials. *J. Solid State Chem.* **1999**, *146*, 114–123. [[CrossRef](#)]
89. Cambon, O.; Yot, P.; Rul, S.; Haines, J.; Philippot, E. Growth and dielectric characterization of large single crystals of GaAsO₄, a novel piezoelectric material. *Solid State Sci.* **2003**, *5*, 469–472. [[CrossRef](#)]
90. Cambon, O.; Haines, J.; Fraysse, G.; Detaint, J.; Capelle, B.; Van der Lee, A. Piezoelectric characterization and thermal stability of a high-performance alpha-quartz-type material, gallium arsenate. *J. Appl. Phys.* **2005**, *97*, 074110. [[CrossRef](#)]
91. Cambon, O.; Bhalerao, G.M.; Bourgogne, D.; Haines, J.; Hermet, P.; Keen, D.A.; Tucker, M.G. Vibrational Origin of the Thermal Stability in the High-Performance Piezoelectric Material GaAsO₄. *J. Am. Chem. Soc.* **2011**, *133*, 8048–8056. [[CrossRef](#)] [[PubMed](#)]
92. Bhalerao, G.M.; Cambon, O.; Haines, J.; Levelut, C.; Mermet, A.; Sirotkin, S.; Menaert, B.; Debray, J.; Baraille, I.; Darrigan, C.; Rerat, M. Brillouin spectroscopy, calculated elastic and bond properties of GaAsO₄. *Inorg. Chem.* **2010**, *49*, 9470–9478. [[CrossRef](#)] [[PubMed](#)]
93. Souleiman, M.; Bhalerao, G.M.; Guillet, T.; Haidoux, A.; Cambon, M.; Levelut, C.; Haines, J.; Cambon, O. Hydrothermal growth of large piezoelectric single crystals of GaAsO₄. *J. Cryst. Growth* **2014**, *397*, 29–38. [[CrossRef](#)]
94. Hermet, P.; Souleiman, M.; Clavier, D.; Hehlen, B.; Levelut, C.; Sans, P.; Haines, J.; Cambon, O. GaAsO₄: A bifunctional material for piezoelectricity and second harmonic generation. *J. Phys. Chem. C* **2015**, *119*, 8459–8464. [[CrossRef](#)]
95. Roncal-Herrero, T.; Rodriguez-Blanco, J.D.; Benning, L.G.; Oelkers, E.H. Precipitation of iron and aluminum phosphates directly from aqueous solution as a function of temperature from 50 to 200 °C. *Cryst. Growth. Des.* **2009**, *9*, 5197–5205. [[CrossRef](#)]
96. Zaghbi, K.; Julien, C.M. Structure and electrochemistry of FePO₄ center dot 2H₂O hydrate. *J. Power Sources* **2005**, *142*, 279–284. [[CrossRef](#)]
97. Smirnov, M.; Mazhenov, N.; Aliouane, N.; Saint-Gregoire, P. Novel features of the alpha-beta phase transition in quartz-type FePO₄ as evidenced by X-ray diffraction and lattice dynamics. *J. Phys. Condens. Mater.* **2010**, *22*, 225403. [[CrossRef](#)] [[PubMed](#)]
98. Liu, H.W. Synthesis of nanorods FePO₄ via a facile route. *J. Nanopart. Res.* **2010**, *12*, 2003–2006. [[CrossRef](#)]
99. Song, Y.N.; Yang, S.F.; Zavalij, P.Y.; Whittingham, M.S. Temperature-dependent properties of FePO₄ cathode materials. *Mater. Res. Bull.* **2002**, *37*, 1249–1257. [[CrossRef](#)]
100. Souleiman, M.; Hermet, P.; Haidoux, A.; Levelut, C.; Haines, J.; Cambon, O. Combined experimental and theoretical Raman scattering studies of alpha-quartz-type FePO₄ and GaPO₄ end members and Ga_{1-x}Fe_xPO₄ solid solutions. *RSC Adv.* **2013**, *3*, 22078–22086. [[CrossRef](#)]
101. Cachau-Herreillat, D.; Bennazha, J.; Goiffon, A.; Ibanez, A.; Philippot, E. X-ray, DTA and crystal growth investigation on AlPO₄-GaPO₄ and AlPO₄-AlAsO₄ systems. *Eur. J. Solid State Inorg. Chem.* **1992**, *29*, 1295.

102. Xia, H. R.; Qin, Z.K.; Yuan, W.; Liu, S.F.; Zou, Z.Q.; Han, J.R. Growth and properties of trigonal aluminium gallium orthophosphate single crystals $\text{Al}_{1-x}\text{Ga}_x\text{PO}_4$. *Cryst. Res. Technol.* **1997**, *32*, 783–788. [[CrossRef](#)]
103. Xia, H.R.; Wang, J.Y.; Li, L.X.; Zou, Z.Q. Growth and Raman scattering of aluminium gallium orthophosphate piezoelectric crystals. *Prog. Cryst. Growth Charact. Mater.* **2000**, *40*, 253–261. [[CrossRef](#)]
104. Barz, R.U.; David, F.; Schneider, J.; Gille, P. Polymorph stability and phase transitions of trigonal $\text{Al}_{1-x}\text{Ga}_x\text{PO}_4$ mixed crystals. *Z. Kristallogr.* **2001**, *216*, 501–508. [[CrossRef](#)]
105. Haines, J.; Cambon, O.; Fraysse, G.; van der Lee, A. An X-ray powder diffraction study of the high temperature phase transitions in alpha-quartz-type AlPO_4 - GaPO_4 solid solutions. *J. Phys. Condens. Mater.* **2005**, *17*, 4463–4474. [[CrossRef](#)]
106. Cambon, O.; Haines, J.; Cambon, M.; Keen, D.A.; Tucker, M.G.; Chapon, L.; Hansen, N.K.; Souhassou, M.; Porcher, F. Effect of Ga content on the instantaneous structure of $\text{Al}_{(1-x)}\text{Ga}_x\text{PO}_4$ solid solutions at high temperature. *Chem. Mater.* **2009**, *21*, 237–246. [[CrossRef](#)]
107. Souleiman, M. Studies of $\text{M}_{(1-x)}\text{M}'_x\text{XO}_4$ Solid Solutions of α -Quartz Homeotypes and Crystal Growth of GaAsO_4 , a Bifunctional Material with Piezoelectric and Non-Linear Optics Properties. Ph.D. Thesis, Université de Montpellier, Montpellier, France, 2013.
108. Souleiman, M.; Cambon, O.; Haidoux, A.; Haines, J.; Levelut, C.; Ranieri, V.; Hazemann, J.L. Study of Ga^{3+} -induced hydrothermal crystallization of an alpha-quartz type $\text{Ga}_{1-x}\text{Fe}_x\text{PO}_4$ single crystal by in-situ X-ray absorption spectroscopy (XAS). *Inorg. Chem.* **2012**, *51*, 11811–11819. [[CrossRef](#)] [[PubMed](#)]
109. Clavier, D. Croissance hydrothermale de monocristaux isotypes du quartz- α , étude des propriétés physiques et recherche de nouvelles solutions solides avec des oxydes du bloc p (Ge, Sn) et du bloc d (Mn, V, Ti). Ph.D. Thesis, Université de Montpellier, Montpellier, France, 2015.



© 2017 by the authors; licensee MDPI, Basel, Switzerland. This article is an open access article distributed under the terms and conditions of the Creative Commons Attribution (CC BY) license (<http://creativecommons.org/licenses/by/4.0/>).